

Effective-Field Theory of Spin Glasses and the Coherent-Anomaly Method. II. Double-Cluster Approximation

Naomichi Hatano¹ and Masuo Suzuki¹

Received June 3, 1991; final August 16, 1991

An improved version of a cluster-effective-field theory for spin glasses, namely the double-cluster approximation, is formulated. The present version is based not on the *self-consistency* condition, but on the *double-cluster-consistency* condition. The advantages of the approximation combined with the coherent-anomaly method are discussed. The critical data of the spin-glass susceptibility are estimated for the two-, three-, and four-dimensional $\pm J$ models.

KEY WORDS: Effective-field theory; double-cluster approximation; spin-glass transition; coherent-anomaly method; nonclassical critical exponent; $\pm J$ model.

1. INTRODUCTION

Since the development of the series-expansion analysis of fractional critical exponents (see ref. 1 for review), mean-field-type theories have rated low, because *each* of them yields only classical exponents. However, the mean-field theory is still important, for it can present a physical picture of the mechanism of even exotic critical phenomena⁽²⁾; it shows vividly how symmetry breaks spontaneously.⁽²⁾

Recently one of the present authors (M.S.) proposed the coherent-anomaly method (CAM).^(3,4) Once a systematic *series* of mean-field or effective-field approximations is constructed, one can estimate nontrivial critical exponents accurately with the CAM by observing how fractional fluctuations emerge in mean-field data. The remaining problem is how to obtain such a series of approximations. The cluster-mean-field theory based

¹ Department of Physics, Faculty of Science, University of Tokyo, Tokyo 113, Japan.

on the self-consistency condition in each cluster, first proposed by Weiss,⁽⁵⁾ has been frequently used.^(3,4,6-9) Another category of effective-field approximation, which is called here the double-cluster approximation (DCA), has been also applied to the CAM in some works.⁽¹⁰⁾ The DCA is based on the double-cluster consistency condition.⁽¹⁰⁾ This equates the relevant local order parameters for two different clusters A and B , that is, $\langle Q^A \rangle = \langle Q^B \rangle$. The DCA itself has a long history.⁽¹¹⁾ The cluster-variational method (see ref. 12 for review) is also equivalent to it in some cases.⁽¹³⁾ Some properties of the DCA favorable to the CAM have been lately explored.⁽¹⁴⁾

In the previous paper⁽⁹⁾ we formulated a cluster-effective-field theory for spin glasses, which is based on the self-consistency condition for each single cluster. In the present paper the DCA for spin glasses is formulated. With the same amount of calculations as in the previous work, the errors of critical-data estimates are remarkably reduced, especially for the three-dimensional $\pm J$ model. The formulation is given in Section 2. In Section 3 the present approximation is compared with the one proposed previously⁽⁹⁾ and advantages of the DCA are explained phenomenologically. In Section 4 the critical data estimated with CAM analyses are presented for the two-, three-, and four-dimensional $\pm J$ models. A discussion on error estimations of critical data is given in the Appendix.

2. DOUBLE-CLUSTER APPROXIMATION

In the present section two kinds of double-cluster approximation (DCA) for spin glasses are formulated.

We consider two clusters $\Omega = A, B$ embedded in a spin-glass system of infinite size, and trace out spin degrees of freedom outside the clusters. Then we obtain the following effective Hamiltonians:

$$\mathcal{H}_{\text{eff}}^{\Omega} \equiv - \sum_{\langle i, j \rangle} J_{ij} \sigma_i^{\Omega} \sigma_j^{\Omega} - \mu_B H \sum_{i \in \Omega} \sigma_i^{\Omega} - \mu_B \sum_{i \in \partial \Omega} H_{\text{eff}}^{\Omega}(i) \sigma_i^{\Omega} \quad (1)$$

as was shown in the previous paper.⁽⁹⁾ The first term of the rhs is the cluster Hamiltonian. The exchange interactions $\{J_{ij}\}$ are distributed in magnitude independently with a common probability distribution $P(J_{ij})$. The second term is the Zeeman energy produced by a magnetic field applied to the bulk of the cluster. The effect of magnetic fields applied to traced-out spins outside the cluster is propagated to the surface of the cluster through the random interactions, and causes the third term of the rhs of (1). Then the effective fields $\{H_{\text{eff}}^{\Omega}(i)\}$ should be considered⁽⁹⁾ to have distribution in magnitude, which originates in the probability distributions

of the traced-out interactions outside the clusters. In the following the angle brackets $\langle \dots \rangle$ denote the thermal average with respect to the Hamiltonian (1), while the square brackets $[\dots]_{\text{av}}$ denote the sample average with respect to the distribution $P(J)$.

In the paramagnetic phase the effective fields are expected to follow⁽¹⁵⁾ the Gaussian distribution, and only the second moments $\{[\langle \sigma^\Omega \rangle^2]_{\text{av}}\}$ and $\{[(H_{\text{eff}}^\Omega)^2]_{\text{av}}\}$ are important.⁽⁹⁾ From this point of view, the following $(|\partial A| + |\partial B|)$ number of parameters are unknown:

$$[H_{\text{eff}}^A(i)^2]_{\text{av}}, \quad \forall i \in \partial A; \quad [H_{\text{eff}}^B(j)^2]_{\text{av}}, \quad \forall j \in \partial B \quad (2)$$

Now we make the *double-cluster-consistency* (DCC) condition to determine the parameters (2) as follows:

$$[\langle \sigma_0^A \rangle^2]_{\text{av}} = [\langle \sigma_0^B \rangle^2]_{\text{av}} \quad (3)$$

$$[\langle \sigma_{i_1}^A \rangle^2]_{\text{av}} = [\langle \sigma_{i_2}^A \rangle^2]_{\text{av}} = \dots = [\langle \sigma_{j_1}^B \rangle^2]_{\text{av}} = [\langle \sigma_{j_2}^B \rangle^2]_{\text{av}} = \dots \quad (4)$$

where σ_0^Ω denotes the spin at the center of the cluster Ω , while $i_1, i_2, \dots \in \partial A$ and $j_1, j_2, \dots \in \partial B$.

As in the previous paper,⁽⁹⁾ the local order parameters $\{[\langle \sigma^\Omega \rangle^2]_{\text{av}}\}$ in the high-temperature phase can be expanded with respect to an applied magnetic field H and the effective fields H_{eff} . In the case that the probability distribution $P(J)$ is symmetric, the expansion yields⁽⁹⁾

$$[\langle \sigma_0^\Omega \rangle^2]_{\text{av}} = \beta^2 \mu_B^2 \sum_{i \in \Omega} [\langle \sigma_0^\Omega \sigma_i^\Omega \rangle_0^2]_{\text{av}} H^2 + \beta^2 \mu_B^2 \sum_{i \in \partial \Omega} [\langle \sigma_0^\Omega \sigma_i^\Omega \rangle_0^2]_{\text{av}} [H_{\text{eff}}^\Omega(i)^2]_{\text{av}} + O(H^4) \quad (5)$$

Here $\langle \dots \rangle_0$ denotes the thermal average with respect to the cluster Hamiltonian (1) with *no* applied and effective fields. Parameters appearing in the condition (4) can also be expressed in terms of similar correlation functions. Substituting these expansions in (3) and (4), we obtain a set of simultaneous equations, which can be written in the following form with the relevant matrix M :

$$M\mathbf{x} = H^2\mathbf{a} + O(H^4) \quad (6)$$

The solution of Eq. (6) determines the parameters (2) as functions of H^2 . At a temperature T_{SG}^D even an infinitesimal H causes finite values of the parameters (2). This instability corresponds to spontaneous symmetry-breaking, i.e., $\det M = 0$ at $T = T_{\text{SG}}^D$. (Here and in the following the super-

script D indicates that the quantity is derived through the DCA.) The approximate spin-glass susceptibility is given by

$$\chi_{\text{SG}}^{\text{D}} \equiv N\mu_{\text{B}}^2(\partial/\partial(H^2))[\langle\sigma_0^A\rangle^2]_{\text{av}}|_{H=0} \quad (7)$$

The expansion (5) and the solution of (6) yield the explicit form of (7), which has a singularity at $T = T_{\text{SG}}^{\text{D}}$.

Instead of (3) and (4), another kind of DCC condition can be made. Assume *ad hoc* that, at the boundary sites of the clusters $\Omega = A, B$, all the effective fields *per free bond* have the same probability distribution. Then the deviations or the second moments of the distributions can be set so that

$$\forall i \in \partial A, \partial B, \quad [H_{\text{eff}}^{\Omega}(i)^2]_{\text{av}} = w_i [(H_{\text{eff}})^2]_{\text{av}} \quad (8)$$

Here w_i is the number of free bonds on the boundary site i . Now in this formulation only one parameter $[(H_{\text{eff}})^2]_{\text{av}}$ is to be determined. Then the following DCC condition is made:

$$[\langle\sigma_0^A\rangle^2]_{\text{av}} = [\langle\sigma_0^B\rangle^2]_{\text{av}} \quad (9)$$

The substitution of the expansion (5) in (9) yields

$$\chi_{\text{SG}}^{\text{D}} = N\beta^2\mu_{\text{B}}^4(\mathcal{F}^A\mathcal{E}^B - \mathcal{F}^B\mathcal{E}^A)/(\mathcal{F}^A - \mathcal{F}^B) \quad (10)$$

$$\mathcal{F}^A = \mathcal{F}^B \quad \text{at} \quad T = T_{\text{SG}}^{\text{D}} \quad (11)$$

where \mathcal{E}^{Ω} and \mathcal{F}^{Ω} denote the center-to-bulk and center-to-surface correlations, respectively, that is,

$$\mathcal{E}^{\Omega} \equiv \sum_{i \in \Omega} [\langle\sigma_0^{\Omega}\sigma_i^{\Omega}\rangle_0^2]_{\text{av}}, \quad \mathcal{F}^{\Omega} \equiv \sum_{i \in \partial\Omega} w_i [\langle\sigma_0^{\Omega}\sigma_i^{\Omega}\rangle_0^2]_{\text{av}} \quad (12)$$

Some other variations of the DCC condition can be made.^(10,14)

3. COMPARISON BETWEEN SINGLE- AND DOUBLE-CLUSTER APPROXIMATIONS

In the present section, two advantages of the DCA over the ordinary single-cluster approximation (SCA) are pointed out.⁽¹⁴⁾

In the previous paper⁽⁹⁾ we formulated the effective-field theory of spin glasses for a single cluster Ω , starting from the *self-consistency condition*⁽⁹⁾ $[\langle\sigma_0\rangle^2]_{\text{av}} = [\langle\sigma_i\rangle^2]_{\text{av}}, \forall i \in \partial\Omega$. To make discussions simple, we treat here another kind of self-consistency condition,

$$[J^2]_{\text{av}} [\langle\sigma_0\rangle^2]_{\text{av}} = \mu_{\text{B}}^2 [(H_{\text{eff}})^2]_{\text{av}} \quad (13)$$

with the assumption (8). This is a straightforward extension of the ordinary mean-field approximation⁽⁵⁾ $J\langle\sigma_0\rangle = \mu_B H_{\text{mf}}$ in ferromagnets. This yields

$$\chi_{\text{SG}}^{\text{S}} = N\beta^2 \mu_B^4 \mathcal{E} / (1 - \beta^2 [J^2]_{\text{av}} \mathcal{F}) \quad (14)$$

$$\mathcal{F} = k_B^2 T^2 / [J^2]_{\text{av}} \quad \text{at } T = T_{\text{SG}}^{\text{S}} \quad (15)$$

where \mathcal{E} and \mathcal{F} are defined by (12). Here and in the following the super-script S denotes the quantity obtained through the SCA. Comparing (15) with (11) yields the following discussion.

The temperature dependence of the center-to-surface correlation (12) for two clusters of different sizes is shown schematically in Fig. 1. At high temperatures where the correlation length $\xi(T)$ is enough less than the cluster size L , the center-to-surface correlation \mathcal{F} can be expressed in the finite-size scaling form,⁽¹⁶⁾

$$\mathcal{F}(T) \equiv \sum_{i \in \partial\Omega} w_i [\langle\sigma_0 \sigma_i\rangle_0^2]_{\text{av}} \simeq \frac{f(L/\xi)}{L^{d-2+\eta}} \times L^{d-1} = L^{1-\eta} f\left(\frac{L}{\xi(T)}\right) \quad (16)$$

where f is the relevant scaling function. The crossing point $\mathcal{F} = k_B^2 T^2 / [J^2]_{\text{av}}$ gives the approximate critical point T_{SG}^{S} by the SCA, or (15). The size dependence of $T_{\text{SG}}^{\text{S}}(L)$ is estimated⁽⁴⁾ as follows:

$$T_{\text{SG}}^{\text{S}}(L) - T_{\text{SG}}^{*\text{S}} \simeq [(a + b \log L)/L]^{1/\nu} \quad (17)$$

Here we have used the scaling form (16) and the relation $\xi(T) \propto (T - T_{\text{SG}}^{*\text{S}})^{-\nu}$, with $T_{\text{SG}}^{*\text{S}}$ denoting the true critical point and a, b appropriate constants. When we select two clusters of the size $L = L_A, L_B$ with $L_A < L_B$, the estimate (17) gives⁽⁴⁾

$$T_{\text{SG}}^{*\text{S}} < T_{\text{SG}}^{\text{S}}(L_B) < T_{\text{SG}}^{\text{S}}(L_A) \quad (18)$$

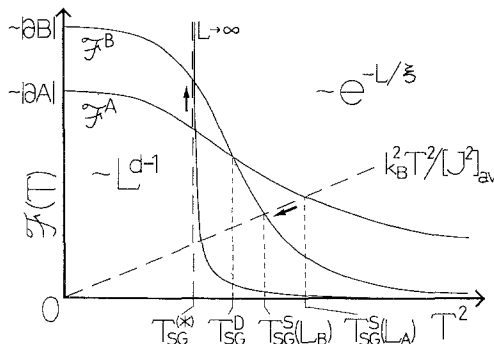


Fig. 1. Temperature dependence of the surface correlation \mathcal{F}^Ω for the clusters $\Omega = A, B$ with their sizes $L_A < L_B$. The behavior in the limit $L \rightarrow \infty$ is also shown.

On the other hand, near the true critical temperature, the correlation length is much greater than the cluster diameter. The center-to-surface correlation is saturated at a value proportional to the surface area of the cluster, L^{d-1} . It grows as we increase the cluster size, i.e.,

$$\mathcal{F}^A < \mathcal{F}^B \quad \text{for } L_A < L_B \ll \xi(T) \quad (19)$$

as is shown in Fig. 1. The crossing point $\mathcal{F}^A = \mathcal{F}^B$ gives the critical temperature $T_{\text{SG}}^{\text{D}}(L_A; L_B)$ in the DCA, or (11). Inequalities (18) and (19) yield

$$T_{\text{SG}}^{(*)} < T_{\text{SG}}^{\text{D}}(L_A; L_B) < T_{\text{SG}}^{\text{S}}(L_B) < T_{\text{SG}}^{\text{S}}(L_A) \quad (20)$$

Then the DCA can yield approximate critical points closer to the true one $T_{\text{SG}}^{(*)}$ than the SCA does, using the same correlation function data.

In the limit of $L \rightarrow \infty$, the center-to-surface correlation \mathcal{F} vanishes in the paramagnetic phase owing to the factor $\exp(-L/\xi)$, while at $T = T_{\text{SG}}^{(*)}$,

$$\mathcal{F} \propto L^{-(d-2+\eta)} \times L^{d-1} = L^{1-\eta} \rightarrow \infty \quad \text{as } L \rightarrow \infty \quad (21)$$

Therefore the approximate transition temperature $T_{\text{SG}}^{\text{D}}(L_A; L_B)$ is expected to approach $T_{\text{SG}}^{(*)}$ as $L_A, L_B \rightarrow \infty$, which can be seen in Fig. 1. For two clusters of sizes close to each other, that is, $|L_A - L_B|/L_B \ll 1$, the phenomenology gives⁽¹⁴⁾

$$T_{\text{SG}}^{\text{D}}(L_A; L_B) - T_{\text{SG}}^{(*)} \simeq (c/L)^{1/\nu} \quad (22)$$

Besides the inequality (20), another advantage of the DCA can be pointed out. From the point of view of the coherent-anomaly method (CAM),^(3,4) attention should be paid to the behavior of the approximation as a systematic *series*. In the CAM, approximation data are fitted to the function^(3,4)

$$\bar{\chi}_{\text{SG}}(L) = C(T_{\text{SG}}(L) - T_{\text{SG}}^{(*)})^{-(\gamma_s-1)} \quad (23)$$

where γ_s denotes the fractional critical exponent of the true spin-glass susceptibility $\chi_{\text{SG}}^{(*)}$, i.e., $\chi_{\text{SG}}^{(*)} \simeq C'(T - T_{\text{SG}}^{(*)})^{-\gamma_s}$. The quantity $\bar{\chi}_{\text{SG}}$ in the lhs of (23) denotes the coherent anomaly, which is defined from the behavior of the approximate spin-glass susceptibility as follows:

$$\chi_{\text{SG}}(T; L) \simeq \bar{\chi}_{\text{SG}}(L) \cdot T_{\text{SG}}(L) / [T - T_{\text{SG}}(L)] \quad (24)$$

near and above $T \simeq T_{\text{SG}}(L)$. It has been pointed out recently,^(7,8) however, that the logarithmic term in the rhs of (17) may prevent one from fitting the data $\{T_{\text{SG}}^{\text{S}}(L)\}$ and $\{\bar{\chi}_{\text{SG}}^{\text{S}}(L)\}$ to the function (23) with desirable

accuracy. Indeed, in the previous paper⁽⁹⁾ we could not obtain a good estimate of the exponent γ_s for the three-dimensional $\pm J$ model owing to the slow convergence of the data. On the contrary, there is no dominant logarithmic term in the DCA (22). Then a series of the DCA for clusters $L_A < L_B < L_C \dots$ fitted to the function (23) can be expected to yield estimates of $T_{SG}^{(*)}$ and γ_s more accurately than a series of the SCA does.

Figure 1 gives a guideline for selecting such a DCA. The first kind of DCA with (3)–(7) works quite well for the ferromagnetic systems and yields transition points even better than the second kind of DCA with (9)–(11). We found, however, that the first kind of DCA (7) for the $\pm J$ model becomes unstable in view of the above guideline, or Fig. 1. For (7) we need to calculate surface-to-surface correlations, which may be strongly affected by the existence of frustrations near the corners of the clusters. Hereafter the second kind of DCA is mainly used. The selection of the clusters was made also under the above guideline.

The appropriately scaled center-to-surface correlation $\mathcal{F}/L^{1-\eta}$ shows the same behavior as does the quantity g_L , which is frequently used in analyzing Monte Carlo data.^(17,18) The essential feature of the CAM is that the system size L does not appear explicitly in (23) owing to the employment of the effective-field theory. The irregularity caused by the shape of the clusters can be screened out effectively. In addition, we need not be concerned about the definition of cluster size. These are the reasons why even small clusters can be used successfully for the CAM-fitting.

4. CAM ANALYSES

In the present section the DCA data are analyzed with the CAM for the two-, three-, and four-dimensional $\pm J$ Ising spin glasses; $P(J) \equiv [\delta(J - J_0) + \delta(J + J_0)]/2$.

4.1. The Two-Dimensional System

It is widely accepted now that the two-dimensional spin glasses with a symmetric distribution of interaction signs exhibit no phase transition at finite temperatures. The exponent of the singularity at zero temperature is well determined⁽¹⁸⁻²¹⁾ as $\gamma_s \sim 5$: The Monte Carlo-simulation studies gave the estimates $\gamma_s = 4.5(5)$,⁽¹⁹⁾ $4.6(5)$,⁽¹⁸⁾ and $5.11(5)$,⁽²¹⁾ while the series-expansion study yielded the estimate $\gamma_s = 5.3(3)$.⁽²⁰⁾ In the previous paper⁽⁹⁾ we also obtained a consistent conclusion.

Here we report the CAM analyses for the DCA data. We assumed the zero-temperature transition. The fitting function is $\bar{\chi}_{SG}^{(n)} \simeq c/(T_{SG}^{(n)})^{\gamma_s - 1}$. The least-squares fitting for the five data points in Table I(a) yields the dashed

line drawn in Fig. 2, or the exponent estimate $\gamma_s = 4.62(12)$. There are, however, systematic deviations of these data points from the dashed line. When we reject the two data points denoted by the open circles in Fig. 2, the last three points give the solid line, or the critical data;

$$\gamma_s = 5.09 \pm 0.09 \quad \text{for} \quad T_{SG}^{(*)} \equiv 0 \quad (25)$$

where the same error estimation as in the previous paper⁽⁹⁾ has been made. To make a comparison, the SCA data given by (13)–(15) are plotted together in Fig. 2. Figure 2 presents an example of the more rapid convergence of (22) as compared to (17).

Table I. The Approximate Transition Temperature $T_{SG}^{(n)}$ and the Critical Amplitude $\bar{\chi}_{SG}^{(n)}$ Obtained with the DCA

Size of the clusters	$T_{SG}^{(n)}$	$\bar{\chi}^{(n)}$
(a) Two-dimensional $\pm J$ model		
2 · 2 – 3 · 3	1.10481	2.48777
2 · 2 – 4 · 3	1.08254	2.75769
3 · 3 – 4 · 3	1.01680	3.74232
3 · 3 – 4 · 4	0.963043	5.16371
4 · 3 – 4 · 4	0.913502	7.17301
(b) Three-dimensional $\pm J$ model ^a		
1 · 1 · 1 – 2 · 1 · 1	2.07808	0.161403
1 · 1 · 1 – 2 · 2 · 1	2.03303	0.187139
2 · 1 · 1 – 2 · 2 · 1	1.99689	0.212842
2 · 1 · 1 – 2 · 2 · 2	1.93167	0.271250
2 · 2 · 1 – 2 · 2 · 2	1.87996	0.335257
2 · 2 · 1 – 3 · 2 · 2	1.87847	0.336528
2 · 2 · 2 – 3 · 2 · 2	1.87699	0.338009
2 · 2 · 2 – 3 · 3 · 2	1.83368	0.402585
3 · 2 · 2 – 3 · 3 · 2	1.79889	0.471621
3 · 2 · 2 – 3 · 3 · 3	1.7440(16)	0.5993(25)
3 · 3 · 2 – 3 · 3 · 3	1.7003(29)	0.7461(66)
(c) Four-dimensional $\pm J$ model		
1 · 1 · 1 · 1 – 2 · 1 · 1 · 1	2.51456	0.100206
1 · 1 · 1 · 1 – 2 · 2 · 1 · 1	2.49370	0.106266
2 · 1 · 1 · 1 – 2 · 2 · 1 · 1	2.47680	0.111639
2 · 1 · 1 · 1 – 2 · 2 · 2 · 1	2.45175	0.120644
2 · 2 · 1 · 1 – 2 · 2 · 2 · 1	2.43198	0.128622
2 · 2 · 1 · 1 – 2 · 2 · 2 · 2	2.40013	0.143636
2 · 2 · 2 · 1 – 2 · 2 · 2 · 2	2.37578	0.157086

^a Here the error bars are due to the random sampling of bond configurations.

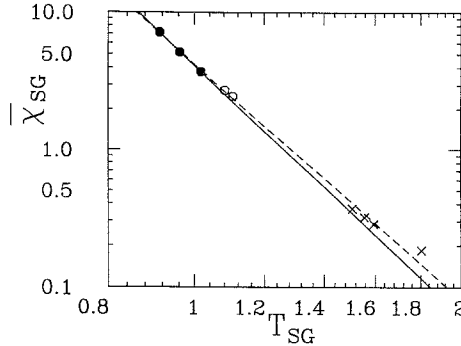


Fig. 2. The CAM fitting for the two-dimensional $\pm J$ model. The DCA data listed in Table I(a) are plotted (● and ○). The dashed line denotes the fitting for these five data points. The solid line denotes the fitting for the last three data points (●). The SCA data are also plotted (×).

4.2. The Three-Dimensional System

The existence of the spin-glass phase transition in the three-dimensional $\pm J$ spin system has been concluded in many works.^(17, 18, 20, 22, 23) The data obtained in the previous paper⁽⁹⁾ also suggest the existence of this transition. The critical data, however, have rather large error bars.

With the DCA we obtained the CAM data listed in Table I(b). The last two data points have error bars owing to the random sampling of bond configurations. The number of the samples is about 2.5×10^5 , where we have used the gauge symmetry.⁽²⁴⁾ These statistical errors were neglected in the fitting because they are comparable to fitting errors. The fitting function used here is⁽⁶⁾

$$\bar{\chi}^{(n)} \simeq c_1 / (T_{SG}^{(n)} - T_{SG}^{(*)})^{\gamma_s - 1} + c_2 / (T_{SG}^{(n)} - T_{SG}^{(*)})^{\gamma_s - 2} \tag{26}$$

where the second term in (26) was added to allow for the behavior away from the critical point. These terms do exist as the Taylor series of an analytic function. As a result of fittings, the second term in (26) is not so small compared to the first. This supports the necessity of the second term in the present case. Singular terms with another fractional exponent θ ($\gamma_s > \theta > \gamma_s - 1$) may also exist,⁽²⁵⁾ which causes the additional term $d / (T_{SG}^{(n)} - T_{SG}^{(*)})^{\theta - 1}$ in (26). This is still an open problem.

The CAM data $\{(T_{SG}^{(n)}, \bar{\chi}_{SG}^{(n)})\}$ can be expressed^(4, 6) in terms of other temperature variables x , e.g., as $\{(K_{SG}^{(n)}, \bar{\chi}_{SG}^{(n)})\}$ with $K \equiv J_0 / k_B T$. Data thus converted were also fitted to the function of the form (26), as in the previous paper.⁽⁹⁾ The critical data thus obtained scatter in a region as is shown in Fig. 3. A discussion about the error analyses of these data is given

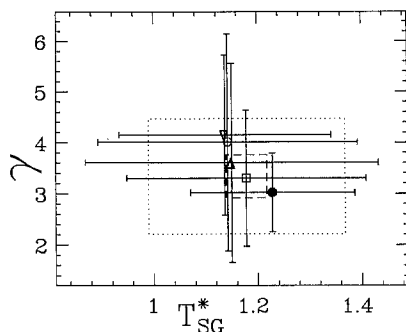


Fig. 3. The critical data obtained in terms of some temperature variables. The variable x is set to $x = T$ (●), $J_0/k_B T$ (○), $\tanh(J_0/k_B T)$ (□), $\tanh^2(J_0/k_B T)$ (△), and $\exp(-J_0/k_B T)$ (▽). The error bars are estimated by the method of least squares. The inner box (---) denotes the error estimates (28); the outer box (···) denotes (27).

in the Appendix. The final estimates [with “error type B,” or (A.6) in the Appendix] are

$$T_{SG}^{(*)} = 1.18 \pm 0.19, \quad \gamma_s = 3.3 \pm 1.1 \quad (27)$$

The error estimates (with “error type A” in the Appendix), which should be compared with the data of the high-temperature expansion⁽²⁰⁾ [$T_{SG}^{(*)} = 1.2(1)$, $\gamma_s = 2.9(5)$], are given by

$$T_{SG}^{(*)} = 1.18 \pm 0.04, \quad \gamma_s = 3.3 \pm 0.4 \quad (28)$$

with the standard deviation (A.3) of the critical data plotted in Fig. 3. Each error bar (28) is below half of the one obtained in the previous paper.⁽⁹⁾

4.3. The Four-Dimensional System

The CAM data for the four-dimensional $\pm J$ model are listed in Table I(c). Because the range of the approximate transition points is narrow, the fitting becomes unstable. The estimate of the exponent deviates appreciably by changing temperature variables x . The transition point, however, can be estimated rather accurately as $T_{SG}^{(*)} = 1.92(7)$. This value is slightly lower than the estimate $T_{SG}^{(*)} = 2.02(6)$ by the high-temperature series analysis.⁽²⁰⁾ We also tested the fitting by *fixing* $T_{SG}^{(*)} \equiv 2.02$. Then the exponent was estimated as $\gamma_s = 2.34(3)$. This result is consistent within error bars with, but slightly greater than, the high-temperature series estimate $\gamma_s = 2.0(4)$. This inconsistency may be due to a systematic error caused by the smallness of the clusters used in the present analysis.

5. SUMMARY

The double-cluster approximation for spin glasses has been formulated. Observing two clusters of slightly different sizes may remind us of the renormalization-group approach.⁽²⁶⁾ The essential difference between the CAM and the renormalization-group scheme is the following^(4,7): In the renormalization-group approach spin degrees of freedom are recursively traced out. In contrast, in the CAM we take account of the degrees of freedom gradually.

The discussion in Section 3 is valid for other phase transitions in view of the super-effective-field theory.⁽²⁾ The DCA-CAM can be an efficient strategy for studying exotic phase transitions.⁽¹⁴⁾

As for $\pm J$ Ising spin glasses, we have confirmed the results obtained by other authors⁽¹⁷⁻²³⁾ in two and three dimensions, while in four dimensions a slight inconsistency was observed between our tentative results and the high-temperature series analysis.⁽²⁰⁾

APPENDIX. ERROR ESTIMATION OF CRITICAL DATA OBTAINED BY CAM ANALYSES

When we obtain critical data from a CAM analysis, there are various ways to estimate the errors of these critical data. In the present appendix, we discuss which estimations should be made.

In the CAM analyses, data points $(T_c^{(1)}, \bar{\chi}^{(1)})$, $(T_c^{(2)}, \bar{\chi}^{(2)})$,... are fitted to the function⁽⁶⁾

$$\bar{\chi}^{(n)} = c_1 |x_c^{(n)} - x_c^{(*)}|^{-(\gamma-1)} + c_2 |x_c^{(n)} - x_c^{(*)}|^{-(\gamma-2)} + \dots \quad (\text{A.1})$$

where the temperature variable x is set equal to T , $J/k_B T$, $\tanh(J/k_B T)$, and so on.^(4,6) [The weak singular terms in the rhs of (A.1) are omitted in many cases.] Then we obtain a set of critical data $(T_{c(x)}^{(*)} \pm \Delta T_{c(x)}^{(*)}$, $\gamma_{(x)} \pm \Delta\gamma_{(x)}$), where the subscript (x) denotes the temperature variable used in the fitting. The situation is schematically shown in Fig. 4(i). The error bars here are estimated from the least-squares fitting.

The first candidate for the error estimates (referred to as error type A in the following) is the standard deviation⁽⁹⁾ of the data $\{\gamma_{(x)}\}$. The final estimate of the value γ_{final} itself is determined in the following form:

$$\gamma_{\text{final}} \equiv \sum_x \frac{\gamma_{(x)}}{(\Delta\gamma_{(x)})^2} \bigg/ \sum_x \frac{1}{(\Delta\gamma_{(x)})^2} \quad (\text{A.2})$$

where \sum_x denotes the summation over the kind of the variables $\{x\}$. The weight $(\Delta\gamma_{(x)})^{-2}$ is introduced here, which represents the reliability of the

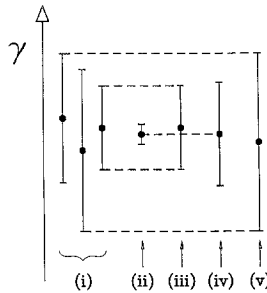


Fig. 4. Some variations of the error estimates of the critical data obtained by the CAM analyses. (i) The original critical data obtained by the method of least squares in terms of some temperature variables $\{x\}$. The error bars here are the fitting errors appearing in the method of least squares. (ii) The average (A.2) with the standard deviation (A.3), which is referred to as error type A in the text. (iii) The most reliable critical data with its fitting error (A.5), which is referred to as error type B. (iv) The average (A.2) with the average of fitting errors (A.6), which is also referred to as error type B. (v) The error bar including all the fitting errors of the original data.

value $\gamma_{(x)}$. The standard deviation is obtained as follows [Fig. 4(ii)] for error type A:

$$(\Delta\gamma_{\text{final}})^2 \equiv \left[\sum_x \frac{\gamma_{(x)}^2}{(\Delta\gamma_{(x)})^2} / \sum_x \frac{1}{(\Delta\gamma_{(x)})^2} \right] - \gamma_{\text{final}}^2 \tag{A.3}$$

The final estimates of the values $T_{c,\text{final}}^{(*)}$ and $\Delta T_{c,\text{final}}^{(*)}$ are determined in the same way. Note that the absolute values of the fitting errors $\{\Delta\gamma_{(x)}\}$ do not affect the final estimates $\Delta\gamma_{\text{final}}$; only their ratios do. This estimate of the error $\Delta\gamma_{\text{final}}$ is interpreted as follows: In the present case the data $\{T_{c(x)}^{(*)}\}$ and $\{\gamma_{(x)}\}$ scatter because of changing the temperature variables x . The variable x can be expressed in terms of another temperature variable x' in the form $x_c - x_c^{(*)} \simeq a(x'_c - x_c'^{(*)}) + b(x'_c - x_c'^{(*)})^2 + \dots$. When we change the temperature variable x in the fitting function (A.1), we effectively allow for less-singular terms. Then the error of type A is caused by the lack of knowledge about the behavior of the coherent anomaly away from the true singular point $T_c^{(*)}$.

The counterpart of the error of type A appears in the Padé analysis, which is usually used for the data obtained by the high-temperature expansion.⁽²⁰⁾ One can make some variations of the Padé approximation by adjusting the number of terms in the numerator and denominator of the Padé approximant:

$$\left(1 + \sum_{n=1}^{N-M} c_n x^n \right) / \left(1 + \sum_{m=1}^M b_m x^m \right) = 1 + \sum_{k=1}^N a_k x^k + O(x^{N+1}) \tag{A.4}$$

Critical data thus obtained scatter within a region. Changing the number M in the Padé approximant (A.4) means changing the coefficients of the higher-order terms $O(x^{N+1})$ in the rhs of (A.4). Then their standard deviation corresponds to the error type A mentioned above. In contrast in the finite-size scaling analyses of Monte Carlo data, one usually assumes^(17-19,21,22) only the most singular term and does not allow for the error of type A.

Another candidate for the error estimation (referred to as error type B in the following) is the use of the absolute values of the fitting errors $\Delta T_{c(x)}^{(*)}$ and $\Delta\gamma_{(x)}$. Some kinds of error type B are defined in the following.

If one interprets the value of $\Delta\gamma_{(x)}$ as the reliability of the value $\gamma_{(x)}$, the most reliable value is the datum $\gamma_{(x_0)}$ whose fitting error $\Delta\gamma_{(x_0)}$ is the minimum among others $\{\Delta\gamma_{(x)}\}$. This leads to the following choice of the final estimates [Fig. 4(iii)]:

$$\text{error type B}_1: \quad \gamma_{\text{final}} = \gamma_{(x_0)}, \quad \Delta\gamma_{\text{final}} = \Delta\gamma_{(x_0)} \quad (\text{A.5})$$

where $\forall x, \Delta\gamma_{(x_0)} \leq \Delta\gamma_{(x)}$. In many cases the choice of the temperature variable $x = T$ minimizes the fitting errors.

Another choice of the estimation of error type B can be made as the “average” of the fitting errors. With the average value defined by (A.2), one estimates its error as follows [Fig. 4(iv)]:

$$\text{error type B}_2: \quad (\Delta\gamma_{\text{final}})^{-2} = \left[\sum_x (\Delta\gamma_{(x)})^{-2} \right] / (N_x - 1) \quad (\text{A.6})$$

where N_x is the number of kinds of temperature variables $\{x\}$.

The largest error bar is determined so as to include all the fitting errors $\Delta T_{c(x)}^{(*)}$ and $\Delta\gamma_{(x)}$ for various variables $\{x\}$ [Fig. 4(v)]. The final estimate of the critical datum itself is obtained as the midpoint value of the error bar. This estimate is too rough, because a shift of the true value by the amount of this error has a fairly small probability.

All the error estimations of type B defined above are based on the fitting errors. Generally speaking, the fitting errors in the method of least squares come from two origins: the irregularity of the fitted data and the finiteness of the number of the data. The former means zigzag behavior of the fitted data, while the latter means that a little shift of fitting parameters does not lead to very bad fits. The error estimates stated in Monte Carlo studies^(17-19,21,22) correspond to the latter. Though the Padé analysis yields no fitting errors, error of the same type exists latently. The error estimation by changing the number of terms of the Padé approximants does not indicate the convergence of the series. If one can calculate higher-order

terms, the critical data may shift beyond the error estimate of type A, which was also noted in ref. 20.

Finally, there may be another source of systematic errors, that is, a nontrivial correction-to-scaling exponent,⁽²⁵⁾ which is mentioned below (26). To include such a term in the analysis, one needs to execute a rather extensive calculation for getting many data points. Because of the limitations of computers, this correction term usually cannot be taken into consideration in CAM analyses⁽⁹⁾ or in finite-size scaling analyses.^(17-19,22)

Summarizing the above discussions, we should note the type of error when we compare the critical data obtained from the CAM analyses with those from other analyses.

ACKNOWLEDGMENTS

We express our sincere gratitude to Prof. Donald D. Betts for various comments and suggestions. We are also grateful to Prof. Hidetoshi Nishimori, Dr. Akira Terai, Dr. Makoto Katori, Naoki Kawashima, and Yoshihiko Nonomura for useful discussions. One of us (N.H.) is grateful to the Nihon-Sekiyu-Kagaku Scholarship for its financial support. The present calculations were performed on the HITAC S820 of the Computer Centre, University of Tokyo, and on the VAX6440 of the Meson Science Laboratory, Faculty of Science, University of Tokyo. We also express our gratitude to Prof. Ryugo Hayano for making available the VAX machine.

REFERENCES

1. C. Domb, On the theory of cooperative phenomena in crystals, *Adv. Phys.* **9**:149-361 (1960).
2. M. Suzuki, Statistical mechanical theory of cooperative phenomena. II. Super-effective-field theory with applications to exotic phase transitions, *J. Phys. Soc. Jpn.* **57**:2310-2330 (1988).
3. M. Suzuki, Statistical mechanical theory of cooperative phenomena. I. General theory of fluctuations, coherent anomalies and scaling exponents with simple application to critical phenomena, *J. Phys. Soc. Jpn.* **55**:4205-4230 (1986).
4. M. Suzuki, M. Katori, and X. Hu, Coherent anomaly method in critical phenomena. I, *J. Phys. Soc. Jpn.* **56**:3092-3112 (1987).
5. P. Weiss, L'hypothèse du champ moléculaire et la propriété ferromagnétique, *J. Phys. Radium* **6**:661-690 (1907).
6. M. Katori and M. Suzuki, Coherent anomaly method in critical phenomena. II. Applications to the two- and three-dimensional Ising models, *J. Phys. Soc. Jpn.* **56**:3113-3125 (1987).
7. A. Patrykiewicz and P. Borowski, Application of the Monte Carlo coherent-anomaly method to two-dimensional lattice-gas systems with further-neighbor interactions, *Phys. Rev. B* **42**:4670-4676 (1990).

8. N. Ito and M. Suzuki, Size dependence of coherent anomalies in self-consistent cluster approximations, *Phys. Rev. B* **43**:3483–3492 (1991).
9. N. Hatano and M. Suzuki, Effective-field theory of spin glasses and the coherent-anomaly method. I, *J. Stat. Phys.* **63**:25–46 (1991).
10. T. Oguchi and H. Kitatani, Coherent-anomaly method applied to the quantum Heisenberg model, *J. Phys. Soc. Jpn.* **57**:3973–3978 (1988); A. Lipowski, Coherent anomaly method with modified Bethe approximation, *J. Magn. Magn. Mat.* **96**:267–274 (1991); Coherent anomaly method with a new mean-field type approximation, *Physica A* **173**:293–301 (1991); Y. Nonomura and M. Suzuki, Coherent-anomaly method in zero-temperature phase transition of quantum spin systems, *J. Phys. A: Math. Gen.* **24** (1991).
11. T. Oguchi and I. Ono, Theory of critical magnetic scattering of neutrons by ferromagnet and antiferromagnet, *J. Phys. Soc. Jpn.* **21**:2178–2193 (1966).
12. D. M. Burley, Closed form approximations for lattice systems, in *Phase Transition and Critical Phenomena*, Vol. 2, C. Comb and M. S. Green, eds. (Academic Press, London, 1972), pp. 329–374.
13. S. Fujiki, M. Katori, and M. Suzuki, Study of coherent anomalies and critical exponents based on high-level cluster-variation approximations, *J. Phys. Soc. Jpn.* **59**:2681–2687 (1990); K. Tanaka, T. Horiguchi, and T. Morita, Coherent-anomaly analysis with cluster variation method for spin-pair correlation function of Ising model on square lattice, *J. Phys. Soc. Jpn.* **60**:2576–2587 (1991).
14. M. Suzuki, New trends in physics of phase transitions, in *Evolutionary Trends in the Physical Sciences—Proceedings of the Yoshio Nishina Centennial Symposium*, M. Suzuki and R. Kubo, eds. (Springer-Verlag, 1991); M. Suzuki, N. Hatano, and Y. Nonomura, Canonicity of the double-cluster approximation in the CAM theory, *J. Phys. Soc. Jpn.* **60**:3990–3992 (1991).
15. F. Matsubara and M. Sakata, Theory of random magnetic mixture. III—Glass-like phase, *Prog. Theor. Phys.* **55**:672–682 (1976); S. Katsura and S. Fujiki, Distribution of spins and the thermodynamic properties in the glass-like (spin glass) phase of random Ising bond models, *J. Phys. C: Solid State Phys.* **12**:1087–1099 (1979).
16. M. E. Fisher and M. N. Barber, Scaling theory for finite-size effects in the critical region, *Phys. Rev. Lett.* **28**:1516–1519 (1972).
17. A. T. Ogielski, Dynamics of three-dimensional Ising spin glasses in thermal equilibrium, *Phys. Rev. B* **32**:7384–7398 (1985).
18. R. N. Bhatt and A. P. Young, Numerical studies of Ising spin glasses in two, three, and four dimensions, *Phys. Rev. B* **37**:5606–5614 (1988).
19. W. L. McMillan, Monte Carlo simulation of the two-dimensional random ($\pm J$) Ising model, *Phys. Rev. B* **28**:5216–5220 (1983).
20. R. R. P. Singh and S. Chakravarty, High-temperature series expansion for spin glasses. II. Analysis of the series, *Phys. Rev. B* **36**:559–566 (1987).
21. J.-S. Wang and R. Swendsen, Low-temperature properties of the $\pm J$ Ising spin glass in two dimensions, *Phys. Rev. B* **38**:4840–4844 (1988).
22. A. T. Ogielski and I. Morgenstern, Critical behavior of three-dimensional Ising spin-glass model, *Phys. Rev. Lett.* **54**:928–931 (1985).
23. J.-S. Wang and R. H. Swendsen, Monte Carlo renormalization-group study of Ising spin glasses, *Phys. Rev. B* **37**:7745–7750 (1988).
24. G. Toulouse, Theory of the frustration effect in spin glasses: I, *Comm. Phys.* **2**:115–119 (1977).
25. F. J. Wegner, Corrections to scaling laws, *Phys. Rev. B* **5**:4529–4536 (1972).
26. K. G. Wilson, Renormalization group and critical phenomena. II. Phase-space cell analysis of critical behavior, *Phys. Rev. B* **4**:3184–3205 (1971).